MEMORANDUM
RM-5244-PR
MARCH 1967

AD 650132

MATHEMATICAL ANALYSIS AND DIGITAL SIMULATION OF THE RESPIRATORY CONTROL SYSTEM

Fred S. Grodins, M.D., Jure Buell and Alex J. Bart

DISTRIBUTION STATEMENT
Distribution of this document is unlimited.

PREFACE

This Memorandum describes a mathematical model of the human respiratory control system. It was supported in part by the National Institutes of Health under the following grants: GM-09608-04; 4-K6-HE 14, 187; and 5-ROI-HE 01626.

Two of the authors are now at the Northwestern University Medical School: F. S. Grodins, M.D., Ph.D., consultant to The RAND Corporation, is a Professor of Physiology, and A. J. Bart is an American Cancer Society Fellow there.

A version of this Memorandum was accepted for publication in the Journal of Applied Physiology.

—v—

ABSTRACT

This Memorandum expresses the basic material balance relationships for the lung-blood-tissue gas transport and exchange system in a set of differential-difference equations containing a number of dependent time delays. Additional equations define the chemical details of transport and acid-base buffering, concentration equilibria, and blood flow behavior. Finally, a control function is included defining the dependence of ventilation upon CSF (H^+), and arterial (H^+) and P_{O_2} at the carotid chemoceptors. A Fortran program was written for convenient digital simulation of the responses of the system to a wide variety of forcings, including CO_2 inhalation, hypoxia at sea level, altitude hypoxia, and metabolic disturbances in acid-base balance. Both dynamic and steady-state behavior of the model were reasonably realistic.

CONTENTS

MATHEMATICAL ANALYSIS AND DIGITAL SIMULATION
OF THE RESPIRATORY CONTROL SYSTEM

1. INTRODUCTION

Although recognition of the basic "closed-loop" nature of the
respiratory control system was certainly implicit in the writings of
Haldane and Priestley [1], the first explicit quantitative formula-
tion was made by Gray in 1945 [2]. His algebraic model was restricted
to the steady-state responses of the system to CO_2 inhalation,
arterial anoxemia, and metabolic disturbances in acid-base balance.
The first dynamic analysis of this system appeared in 1954 [3], and
although it represented a step forward in considering dynamics, it
also represented a step backward in that it could accept only a
single forcing, i.e., CO_2 inhalation. It also represented an over-
simplified treatment that nevertheless led to nonlinear differential
equations. At the time of its formulation, the state of the computer
art was relatively primitive, and exploration of a more general and
realistic model was not practical.

With the development of large computing facilities, interest
in the realistic dynamic analysis of complex multivariate biological
control systems has increased rapidly [4]. Beginning with Defares,
Derkson, and Duyff in 1960 [5], the original dynamic model of the
respiratory system has been refined and extended by several workers
using both analog and digital simulation [6-9]. The present analysis
represents a further step in this continuing study. The model has
been made sufficiently general to accommodate a variety of forcings
(CO_2 inhalation, hypoxia at sea level or at altitude, metabolic
disturbances in acid-base balance, or combinations thereof). It
treats the chemical buffering and gas transport systems in reason-
able detail, including both Haldane and Bohr effects, and it

recognizes the presence of many transport delays that are themselves dependent variables. It permits convenient exploration of a variety of possible control functions, including the role of cerebrospinal fluid (CSF) hydrogen ion concentration, and of O_2-CO_2 interaction at the peripheral chemoceptors. Some of these features, particularly the buffer equations and the many dependent time delays, introduce formidable computational difficulties, which have oe^ overcome in the digital simulation herein described.

2. GENERAL DESCRIPTION OF THE SYSTEM

We consider two major components, a controlled system ('plant' or 'process'), and a controlling system (controller).

2.1. Controlled System

The 'plant' comprises three major compartments (lung, brain, tissue) connected by the circulating blood (Fig. 1). The brain compartment is separated from a cerebrospinal fluid reservoir by a membrane of restricted permeability. The events of the respiratory cycle are ignored and the lungs regarded as a box of constant volume, uniform content, and zero dead space ventilated by a continuous uni-directional stream of gas. If the alveolar RQ differs from unity, as it generally will, the rates of flow of inspired and expired gas will differ. We assume that alveolar gas tensions, $P_{A(CO_2)}$, $P_{A(O_2)}$, and $P_{A(N_2)}$ are equal at every instant to those in expired air and arterial blood leaving the lung. The total oxygen content of this arterial blood, $C_{a(O_2)}$, will be the sum of physically dissolved and chemically combined (i.e., oxyhemoglobin) components. The former varies linearly with $P_{a(O_2)}$, whereas the latter is a complex function of both $P_{a(O_2)}$ and arterial blood pH (oxygen dissociation curve including Bohr effect [10]). Similarly, the total CO_2 content of
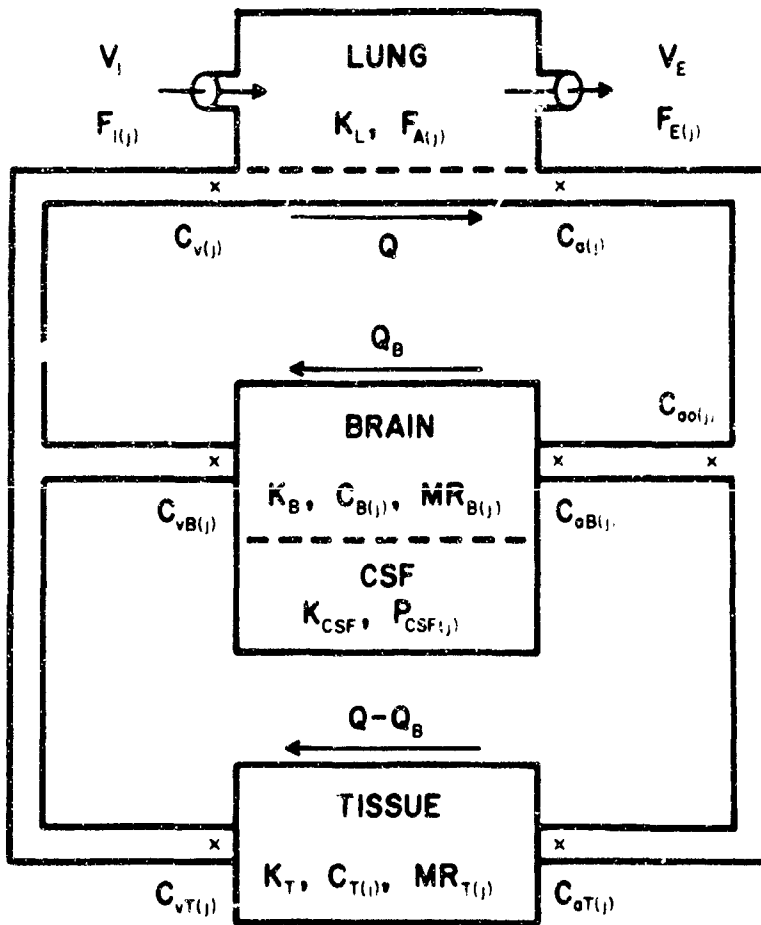
Fig. 1—The controlled system.

(Symbols defined in App. A.)

this blood, $C_{a(CO_2)}$, will comprise both physically dissolved and chemically combined components, the former varying linearly with $P_{a(CO_2)}$ and the latter being a complex implicit function of $P_{a(CO_2)}$, the standard bicarbonate content, $(BHCO_3)_b$, the total hemoglobin and oxyhemoglobin contents (Hb, HbO_2), and the plasma protein content (CO_2 absorption curve including Haldane effect [10]). Carbamate is not explicitly treated as a separate entity. The pH of this blood will depend upon its $P_{a(CO_2)}$ and bicarbonate content as defined by the Henderson-Hasselbalch equation. Only physically dissolved nitrogen will be present.

After a transport delay, which depends upon vascular volume and blood flow rate, this arterial blood arrives at the brain or tissue compartment. We regard the gas tensions in each of these reservoirs as uniform and equal to those in exiting venous blood. Oxygen is removed from and CO_2 is added to each reservoir at a constant rate set by metabolism. The oxygen and nitrogen contents of these reservoirs are taken to include only physically dissolved gas, but the total CO_2 content will include a bicarbonate component in accordance with the CO_2 absorption curve for that reservoir. No Haldane effect is attributed to the reservoirs' CO_2 buffers. Although we assume reservoir-venous blood equality for CO_2 tension, the bicarbonate and hydrogen-ion concentrations will not necessarily be the same. We do not attempt to treat this "effective impermeability" in any rigorous physico-chemical fashion [11], but simply reserve the right to restrict the movement of certain chemical species between the reservoirs and the blood. In this way, for example, we can simulate the limited availability of brain and CSF bicarbonate for buffering strong acid introduced into the blood, a feature of the "blood-brain barrier."

The brain compartment communicates with a cerebrospinal fluid reservoir via a membrane permeable to respiratory gases only. The latter diffuse across this membrane at rates proportional to their tension gradients. The entire gradient occurs across the membrane, the reservoir concentrations being regarded as uniform. The CSF reservoir differs from the brain compartment in containing no protein capable of buffering carbonic acid. For our purposes we regard it simply as a solution of sodium bicarbonate whose bicarbonate content thus remains constant at all CO_2 tensions above 10 mm Hg [10].

Venous blood leaving the brain combines with that leaving the tissue after appropriate time delays to form mixed venous blood, which after another delay, enters the lung to complete the circle of the gas transport and exchange process. Total cardiac output as well as the local blood flow to the brain are known to vary as functions of arterial CO_2 and oxygen tensions [12-16]. Since circulatory transport delays are functions of blood flow rates, these delays become dependent variables as $P_{a(CO_2)}$ and $P_{a(O_2)}$ change in response to such forcings as CO_2 inhalation or hypoxia. These delays are treated as pure dead times, which implies a square blood flow front with no intravascular "smearing."

2.2. Controlling System

This includes receptor elements that monitor concentrations of certain chemical species at particular locations, afferent nerves that transmit this information to the central nervous system, the neural centers themselves, motor nerves to the respiratory muscles, the muscles themselves, and finally the thorax-lung pump which they drive. As in our original model as well as those that have followed it, we shall not attempt to describe this system in terms of the details of its components but instead will go directly from chemical

concentrations at receptor sites as the inputs to ventilation as the output. In so doing, we shall assign no dynamic elements to this system, thus implying that any delays associated with it are negligibly short compared to those of the "plant." This is certainly true of the neural components and probably of the mechanical elements as well.

3. EQUATIONS OF THE SYSTEM

Using symbols and units defined in App. A and "normal" parameter values given in App. B, we first write material balance equations for CO_2, O_2, and N_2 for each of the three compartments, lung, brain, and tissue:

$$\dot{F}_{A(CO_2)} = \frac{1}{K_L}\left[V_I F_{I(CO_2)} - V_E F_{A(CO_2)} + \left(\frac{863}{B-47}\right)Q\left(C_{v(CO_2)} - C_{a(CO_2)}\right)\right] \quad (1.1)$$

$$\dot{F}_{A(O_2)} = \frac{1}{K_L}\left[V_I F_{I(O_2)} - V_E F_{A(O_2)} + \left(\frac{863}{B-47}\right)Q\left(C_{v(O_2)} - C_{a(O_2)}\right)\right] \quad (1.2)$$

$$\dot{F}_{A(N_2)} = \frac{1}{K_L}\left[V_I F_{I(N_2)} - V_E F_{A(N_2)} + \left(\frac{863}{B-47}\right)Q\left(C_{v(N_2)} - C_{a(N_2)}\right)\right] \quad (1.3)$$

$$\dot{C}_{B(CO_2)} = \frac{1}{K_B}\left[MR_{B(CO_2)} + Q_B\left(C_{aB(CO_2)} - C_{vB(CO_2)}\right) - D_{CO_2}\left(P_{B(CO_2)} - P_{CSF(CO_2)}\right)\right] \quad (1.4)$$

$$\dot{C}_{B(O_2)} = \frac{1}{K_B}\left[-MR_{B(O_2)} + Q_B\left(C_{aB(O_2)} - C_{vB(O_2)}\right) - D_{O_2}\left(P_{B(O_2)} - P_{CSF(O_2)}\right)\right] \quad (1.5)$$

$$\dot{C}_{B(N_2)} = \frac{1}{K_B}\left[Q_B\left(C_{aB(N_2)} - C_{vB(N_2)}\right) - D_{N_2}\left(P_{B(N_2)} - P_{CSF(N_2)}\right)\right] \quad (1.6)$$

$$\dot{C}_{T(CO_2)} = \frac{1}{K_T}\left[MR_{T(CO_2)} + (Q-Q_B)\left(C_{aT(CO_2)} - C_{vT(CO_2)}\right)\right] \quad (1.7)$$

$$\dot{C}_{T(O_2)} = \frac{1}{K_T}\left[-MR_{T(O_2)} + (Q-Q_B)\left(C_{aT(O_2)} - C_{vT(O_2)}\right)\right] \quad (1.8)$$

$$\dot{C}_{T(N_2)} = \frac{1}{K_T}\left[(Q-Q_B)\left(C_{aT(N_2)} - C_{vT(N_2)}\right)\right] \quad (1.9)$$

The balance (or diffusion) equations for the CSF subcompartment are written in terms of gas tensions:

$$\dot{P}_{CSF(CO_2)} = \left(D_{CO_2}/K_{CSF}k\alpha_{CSF(CO_2)}\right)\left(P_{B(CO_2)}-P_{CSF(CO_2)}\right) \tag{1.10}$$

$$\dot{P}_{CSF(O_2)} = \left(D_{O_2}/K_{CSF}k\alpha_{CSF(O_2)}\right)\left(P_{B(O_2)}-P_{CSF(O_2)}\right) \tag{1.11}$$

$$\dot{P}_{CSF(N_2)} = \left(D_{N_2}/K_{CSF}k\alpha_{CSF(N_2)}\right)\left(P_{B(N_2)}-P_{CSF(N_2)}\right) \tag{1.12}$$

By adding Eqs. (1.1)–(1.3), noting that the volumetric fractions of CO_2, O_2, and N_2 must add to one in both inspired and alveolar air, and that the sum, $\dot{F}_{A(CO_2)} + \dot{F}_{A(O_2)} + \dot{F}_{A(N_2)}$, must equal zero since the lung volume is constant, we can express V_E in terms of V_I:

$$V_E = V_I + \left(\frac{863}{B-47}\right) Q\left[\left(C_{v(CO_2)}-C_{a(CO_2)}\right) + \left(C_{v(O_2)}-C_{a(O_2)}\right) + \left(C_{v(N_2)}-C_{a(N_2)}\right)\right] \tag{2.1}$$

We now define alveolar–arterial concentration equilibria for CO_2, O_2, and N_2. For CO_2:

$$C_{a(CO_2)} = (BHCO_3)_b + 0.375\left[(Hb)-C_{a(HbO_2)}\right] - \left[0.16 + 2.3(Hb)\right]$$

$$\left[\log\left(\frac{C_{a(CO_2)}-k\alpha_{CO_2}(B-47)F_{A(CO_2)}}{0.01(B-47)F_{A(CO_2)}}\right) - 0.1\right]$$

$$+ k\alpha_{CO_2}(B-47)F_{A(CO_2)} \tag{3.1}$$

For O_2:

$$C_{a(O_2)} = k\alpha_{O_2}(B-47)F_{A(O_2)} + C_{a(HbO_2)}, \tag{3.2}$$

where

$$C_{a(HbO_2)} = (Hb) \left[1 - \exp(-S(B-47)F_{A(O_2)}) \right]^2, \qquad (3.3)$$

$$S = 0.44921(pH_a) - 0.10098 (pH_a)^2 + 0.0066815 (pH_a)^3 - 0.454, \qquad (3.4)$$

$$pH_a = 9 - \log C_{a(H^+)}, \qquad (3.5)$$

and

$$C_{a(H^+)} = K' \left[\frac{k\alpha_{CO_2}(B-47)F_{A(CO_2)}}{C_{a(CO_2)} - k\alpha_{CO_2}(B-47)F_{A(CO_2)}} \right] . \qquad (3.6)$$

Thus Eq. (3.1) is the CO_2 buffer equation including the Haldane effect [2, 10], and Eq. (3.3) is the O_2 dissociation curve including the Bohr effect. Equations (3.3) and (3.4) were fitted empirically to standard data on human blood [17].

For N_2, we have simply:

$$C_{a(N_2)} = k\alpha_{N_2}(B-47)F_{A(N_2)}. \qquad (3.7)$$

We next define venous blood-brain equilibria for CO_2, O_2, and N_2 in terms of gas tensions. For CO_2:

$$C_{B(CO_2)} = (BHCO_3)_B - 0.62 \left[\log \left(\frac{C_{B(CO_2)} - k\alpha_{B(CO_2)} P_{B(CO_2)}}{0.01 \ P_{B(CO_2)}} \right) - 0.14 \right]$$

$$+ k\alpha_{B(CO_2)} P_{B(CO_2)}, \qquad (4.1)$$

and

$$C_{vB(CO_2)} = (BHCO_3)_b + 0.375 \left[(Hb)-C_{vB(HbO_2)}\right] - \left[0.16 + 2.3(Hb)\right]$$

$$\left[\log\left(\frac{C_{vB(CO_2)}-k\alpha_{CO_2}P_{B(CO_2)}}{0.01 \, P_{B(CO_2)}}\right) - 0.14\right] + k\alpha_{CO_2}P_{B(CO_2)}. \quad (4.2)$$

Equation (4.1) is a modified CO_2 buffer relation for brain with the Hb and HbO_2 effects removed, and Eq. (4.2) is the same form as Eq. (3.1). For O_2:

$$C_{vB(O_2)} = \frac{\alpha_{O_2}}{\alpha_{B(O_2)}} \, C_{B(O_2)} + C_{vB(HbO_2)}, \quad (4.3)$$

where as before

$$C_{vB(HbO_2)} = (Hb) \left[1 - \exp\left(-S(C_{B(O_2)}/k\alpha_{B(O_2)})\right)\right]^2;$$

$$C_{B(O_2)} = k\alpha_{B(O_2)}P_{B(O_2)}, \quad (4.4)$$

$$S = 0.44921(pH_{vB}) - 0.10098(pH_{vB})^2 + 0.0066815(pH_{vB})^3 - 0.454, \quad (4.5)$$

$$pH_{vB} = 9 - \log C_{vB(H^+)}, \quad (4.6)$$

and

$$C_{vB(H^+)} = K' \left[\frac{k\alpha_{CO_2}P_{B(CO_2)}}{C_{vB(CO_2)}-k\alpha_{CO_2}P_{B(CO_2)}}\right]. \quad (4.7)$$

Equations similar to (4.6) and (4.7) with C_{vB} replaced by C_B will yield $C_{B(H^+)}$ and pH_B.

For N_2, we have simply:

$$C_{vB(N_2)} = \frac{\alpha_{N_2}}{\alpha_{B(N_2)}} \, C_{B(N_2)};$$

$$C_{B(N_2)} = k\alpha_{B(N_2)} P_{B(N_2)} \tag{4.8}$$

An exactly analogous set of equations with values for the tissue reservoir (subscript T) and tissue venous blood (subscript vT) substituted for those of the brain and brain venous blood is used to define venous—tissue equilibria for CO_2, O_2, and N_2. We will not bother to rewrite them but simply reserve the equation numbers [Eqs. (5.1)—(5.8)] to designate them.

We note here that the hydrogen—ion concentration in CSF, which we will need as an input to the controller, is given by:

$$C_{CSF(H^+)} = K'\left[\frac{k\alpha_{CSF(CO_2)} P_{CSF(CO_2)}}{(BHCO_3)_{CSF}}\right], \tag{6.1}$$

and

$$pH_{CSF} = 9 - \log C_{CSF(H^+)}. \tag{6.2}$$

We next define the dependence of cardiac output and brain blood flow on arterial CO_2 and O_2 tensions using information from the literature [12—16] and assigning an arbitrary first—order lag to the responses. For cardiac output, we have:

$$\dot{Q} = (f_Q - Q)/r_1, \tag{7.1}$$

where

$$f_Q = Q_N + \Delta Q_{(O_2)} + \Delta Q_{(CO_2)}. \tag{7.2}$$

For $X \equiv (B-47)F_{A(O_2)} \approx P_{a(O_2)}$, and $X < 104$, we have:

$$\Delta Q_{(O_2)} = 9.6651 - 0.2885X + (2.9241E-3)X^2 - (1.0033E-5)X^3 \quad (7.3)^*$$

And for $X \geq 104$:

$$\Delta Q_{(O_2)} = 0. \tag{7.4}$$

For $Y \equiv (B-47)F_{A(CO_2)} \approx P_{a(CO_2)}$, and $40 \leq Y \leq 60$,

$$\Delta Q_{(CO_2)} = 0.3(Y - 40), \tag{7.5}$$

And for all other values of Y,

$$\Delta Q_{(CO_2)} = 0. \tag{7.6}$$

For brain blood flow, we have:

$$\dot{Q}_B = (f_{Q_B} - Q_B)/r_2, \tag{7.7}$$

where

$$f_{Q_B} = Q_{BN} + \Delta Q_{B(O_2)} + \Delta Q_{B(CO_2)}. \tag{7.8}$$

---

*"Floating point" notation, i.e.: $E - n \equiv \times 10^{-n}$, in this and subsequent equations.

For X < 104:

$$\Delta Q_{B(O_2)} = 2.785 - 0.1323X + (2.6032E-3)X^2 \\ - (2.324E-5)X^3 + (7.6559E-8)X^4,$$ (7.9)

And for X ≥ 104:

$$\Delta Q_{B(O_2)} = 0.$$ (7.10)

For Y < 38:

$$\Delta Q_{B(CO_2)} = (2.323E-2) - (3.1073E-2)Y \\ + (8.0163E-4)Y^2$$ (7.11)

For 38 ≤ Y ≤ 44:

$$\Delta Q_{B(CO_2)} = 0,$$ (7.12)

And for Y > 44:

$$\Delta Q_{B(CO_2)} = -15.58 + 0.7607Y - (1.2947E-2)Y^2 \\ + (9.3918E-5)Y^3 - (2.1748E-7)Y^4.$$ (7.13)

In each case, the polynomials in X or Y represent empirical fits to data taken from the literature, data admittedly incomplete in several details.

We now express the arterial concentrations of CO_2, O_2, and N_2 at the entrance of the brain, and of the tissue reservoirs—in terms of their concentrations in arterial blood leaving the lungs at an appropriate time in the past, i.e., at "lag time" $(t - \tau)$, where τ is the blood transport delay:

$$C_{aB(CO_2)}(t) = C_{a(CO_2)}(t-\tau_{aB}) \tag{8.1}$$

$$C_{aB(O_2)}(t) = C_{a(O_2)}(t-\tau_{aB}) \tag{8.2}$$

$$C_{aB(N_2)}(t) = C_{a(N_2)}(t-\tau_{aB}) \tag{8.3}$$

$$C_{aT(CO_2)}(t) = C_{a(CO_2)}(t-\tau_{aT}) \tag{8.4}$$

$$C_{aT(O_2)}(t) = C_{a(O_2)}(t-\tau_{aT}) \tag{8.5}$$

$$C_{aT(N_2)}(t) = C_{a(N_2)}(t-\tau_{aT}) \tag{8.6}$$

and in similar fashion, we express the mixed venous concentrations entering the lung in terms of concentrations in venous blood leaving the brain and tissue reservoirs at appropriate lag times:

$$C_{v(CO_2)}(t) = \frac{1}{Q}\left[Q_B(C_{vB(CO_2)}(t-\tau_{vB})) + (Q-Q_B)(C_{vT(CO_2)}(t-\tau_{vT}))\right]$$

$$\tag{8.7}$$

$$C_{v(O_2)}(t) = \frac{1}{Q}\left[Q_B(C_{vB(O_2)}(t-\tau_{vB})) + (Q-Q_B)(C_{vT(O_2)}(t-\tau_{vT}))\right]$$

$$\tag{8.8}$$

$$C_{v(N_2)}(t) = \frac{1}{Q}\left[Q_B(C_{vB(N_2)}(t-\tau_{vB})) + (Q-Q_B)(C_{vT(N_2)}(t-\tau_{vT}))\right]$$

$$\tag{8.9}$$

The variables defined by Eqs. (8.1)-(8.9) will be called "lag variables" for convenience.

Finally we note that the transport delays are not constant but vary with blood flow rates as defined below:

$$\tau_{aB} = \frac{1.062}{\frac{1}{\tau_{aB} - \tau_{aB(1)}} \int_{t-\tau_{aB}}^{t-\tau_{aB(1)}} Q \, dt} + \frac{0.015}{\frac{1}{\tau_{aB(1)}} \int_{t-\tau_{aB(1)}}^{t} Q_B \, dt} \qquad (8.10)$$

$$\tau_{aT} = \frac{1.062}{\frac{1}{\tau_{aT} - \tau_{aT(1)}} \int_{t-\tau_{aT}}^{t-\tau_{aT(1)}} Q \, dt} + \frac{0.735}{\frac{1}{\tau_{aT(1)}} \int_{t-\tau_{aT(1)}}^{t} (Q-Q_B) \, dt} \qquad (8.11)$$

$$\tau_{vb} = \frac{0.06}{\frac{1}{\tau_{vB} - \tau_{vB(1)}} \int_{t-\tau_{vB}}^{t-\tau_{vB(1)}} Q_B \, dt} + \frac{0.188}{\frac{1}{\tau_{vB(1)}} \int_{t-\tau_{vB(1)}}^{t} Q \, dt} \qquad (8.12)$$

$$\tau_{vT} = \frac{2.94}{\frac{1}{\tau_{vT} - \tau_{vT(1)}} \int_{t-\tau_{vT}}^{t-\tau_{vT(1)}} (Q-Q_B) \, dt} + \frac{0.188}{\frac{1}{\tau_{vT(1)}} \int_{t-\tau_{vT(1)}}^{t} Q \, dt} \qquad (8.13)$$

$$\tau_{ao} = \frac{1.062}{\frac{1}{\tau_{ao} - \tau_{ao(1)}} \int_{t-\tau_{ao}}^{t-\tau_{ao(1)}} Q \, dt} + \frac{0.008}{\frac{1}{\tau_{ao(1)}} \int_{t-\tau_{ao(1)}}^{t} Q_B \, dt} \qquad (8.14)$$

The last value, τ_{ao}, which does not appear in Eqs. (8.1)-(8.9), is the lung-to-carotid body delay and will be used in the controller function. In each equation, the numerator represents the volume of the appropriate vascular segment through which blood flows at the appropriate "past-average rate" defined by the denominator.

We have now written all of the relationships required to define the open-loop operation of the isolated "plant." To close the loops, it remains to write a controller function. A major purpose of our simulation is to explore the implications of a variety of such functions, and so far we have looked at two:

$$V_I = 1.1 \ C_{B(H^+)} + 1.31 \ P_{B(CO_2)} + TERM - V_{I(1)}, \tag{9.1}$$

and

$$V_I = 1.138 \ C_{CSF(H^+)} + 1.154 \ C_{a(H^+)}(t-\tau_{ao}) + TERM - V_{I(2)} \tag{9.2}$$

$$TERM \equiv (23.6E-9)\left[104-(B-47)F_{A(O_2)}(t-\tau_{ao})\right]^{4.9}$$

$$\text{for } (B-47)F_{A(O_2)}(t-\tau_{ao}) < 104, \tag{9.3}$$

$$TERM \equiv 0 \qquad \text{for } (B-47)F_{A(O_2)}(t-\tau_{ao}) \geq 104, \tag{9.4}$$

and $V_{I(n)}$ are constants so adjusted that $P_{A(CO_2)} \simeq 40.0$ at rest, breathing air at sea level (standard control point). Equation (9.1) is similar to that used in our earlier model, whereas Eq. (9.2) incorporates recent findings on the roles of CSF and peripheral receptors [18-21]. Neither includes an O_2-CO_2 interaction term, but this as well as a variety of other possibilities can easily be introduced.

4. SOLUTION OF SYSTEM EQUATIONS BY DIGITAL COMPUTER

The equations were programmed for solution on IBM 7044 and CDC 3400 digital computers. For this purpose, the basic material balance equations [Eqs. (1.1)-(1.9)] were rewritten as differential-difference equations with variable time delays, using the appropriate

interrelationship equations developed above:

$$\dot{F}_{A(CO_2)} = \frac{1}{K_L}\left[V_I F_{I(CO_2)} - V_E F_{A(CO_2)} + \left(\frac{863}{B-47}\right)\left(Q_B C_{vB(CO_2)}(t-\tau_{vB})\right.\right.$$
$$\left.\left. + (Q-Q_B)C_{vT(CO_2)}(t-\tau_{vT}) - Q\,C_{a(CO_2)}\right)\right] \tag{10.1}$$

$$\dot{F}_{A(O_2)} = \frac{1}{K_L}\left[V_I F_{I(O_2)} - V_E F_{A(O_2)} + \left(\frac{863}{B-47}\right)\left(Q_B C_{vB(O_2)}(t-\tau_{vB})\right.\right.$$
$$\left.\left. + (Q-Q_B)C_{vT(O_2)}(t-\tau_{vT}) - Q\left(k\alpha_{O_2}(B-47)F_{A(O_2)} + C_{a(HbO_2)}\right)\right)\right] \tag{10.2}$$

$$\dot{F}_{A(N_2)} = \frac{1}{K_L}\left[V_I F_{I(N_2)} - V_E F_{A(N_2)} + \left(\frac{863}{B-47}\right)\left(Q_B C_{vB(N_2)}(t-\tau_{vB})\right.\right.$$
$$\left.\left. + (Q-Q_B)C_{vT(N_2)}(t-\tau_{vT}) - Q\left(k\alpha_{N_2}(B-47)F_{A(N_2)}\right)\right)\right] \tag{10.3}$$

$$\dot{C}_{B(CO_2)} = \frac{1}{K_B}\left[MR_{B(CO_2)} + Q_B\left(C_{a(CO_2)}(t-\tau_{aB}) - C_{vB(CO_2)}\right)\right.$$
$$\left. - D_{CO_2}\left(P_{B(CO_2)} - P_{CSF(CO_2)}\right)\right] \tag{10.4}$$

$$\dot{C}_{B(O_2)} = \frac{1}{K_B}\left[-MR_{B(O_2)} + Q_B\left(\left(k\alpha_{O_2}(B-47)F_{A(O_2)} + C_{a(HbO_2)}\right)(t-\tau_{aB})\right.\right.$$
$$\left.\left. - \left(\frac{\alpha_{O_2}}{\alpha_{B(O_2)}}\right)C_{B(O_2)} - C_{vB(HbO_2)}\right) - D_{O_2}\left(P_{B(O_2)} - P_{CSF(O_2)}\right)\right] \tag{10.5}$$

$$\dot{C}_{B(N_2)} = \frac{1}{K_B}\left[Q_B\left(k\alpha_{N_2}(B-47)F_{A(N_2)}(t-\tau_{aB}) - \left(\frac{\alpha_{N_2}}{\alpha_{B(N_2)}}\right)C_{B(N_2)}\right) - D_{N_2}\left(P_{B(N_2)}-P_{CSF(N_2)}\right)\right] \tag{10.6}$$

$$\dot{C}_{T(CO_2)} = \frac{1}{K_T}\left[MR_{T(CO_2)} + (Q-Q_B)\left(C_{a(CO_2)}(t-\tau_{aB}) - C_{vT(CO_2)}\right)\right] \tag{10.7}$$

$$\dot{C}_{T(O_2)} = \frac{1}{K_T}\left[-MR_{T(O_2)} + (Q-Q_B)\left\{\left(k\alpha_{O_2}(B-47)F_{A(O_2)} + C_{a(HbO_2)}\right)(t-\tau_{aT}) - \left(\frac{\alpha_{O_2}}{\alpha_{T(O_2)}}\right)C_{T(O_2)}-C_{vT(HbO_2)}\right\}\right] \tag{10.8}$$

$$\dot{C}_{T(N_2)} = \left((Q-Q_B)/K_T\right)\left[\left(k\alpha_{N_2}(B-47)F_{A(N_2)}\right)(t-\tau_{aT}) - \left(\frac{\alpha_{N_2}}{\alpha_{T(N_2)}}\right)C_{T(N_2)}\right] \tag{10.9}$$

Equation (2.1) defining V_E in terms of V_I was also rewritten to incorporate the appropriate lag times:

$$V_E = V_I + \left(\frac{863}{B-47}\right)\left(Q_B\left[\left(C_{vB(CO_2)} + C_{vB(O_2)} + C_{vB(N_2)}\right)(t-\tau_{vB})\right]\right.$$
$$+ (Q-Q_B)\left[\left(C_{vT(CO_2)} + \left(\frac{\alpha_{O_2}}{\alpha_{T(O_2)}}\right)C_{T(O_2)} + C_{vT(HbO_2)} + \right.\right.$$
$$\left.\left. + \left(\frac{\alpha_{N_2}}{\alpha_{T(N_2)}}\right)C_{T(N_2)}\right)(t-\tau_{vT})\right]$$
$$\left. - Q\left[C_{a(CO_2)} + k\alpha_{O_2}(B-47)F_{A(O_2)} + C_{a(HbO_2)} + k\alpha_{N_2}(B-47)F_{A(N_2)}\right]\right) \tag{11.1}$$

Methods for the numerical integration of such differential-difference equations with several time lags have been considered in detail elsewhere [22-24]. Here we shall only point out certain special features of the present program that deserve comment.

The first concerns the calculation of current values for $C_{a(CO_2)}$, $C_{a(HbO_2)}$, $C_{vB(CO_2)}$, $C_{vB(HbO_2)}$, $C_{vT(CO_2)}$, and $C_{vT(HbO_2)}$ to put into this system of equations. Special problems are involved here because of the interdependence of CO_2 content, oxyhemoglobin content, and pH, and because of the fact that the buffer equation cannot be solved explicitly for the desired variable. Let us examine the procedure used here. Starting with the current value of $F_{A(CO_2)}$ and a trial guess for $C_{a(CO_2)}$ (say $C_{a(CO_2)(1)}$), we calculate $C_{a(H^+)(1)}$ and $pH_{a(1)}$ from Eqs. (3.6) and (3.5). Putting this value of $pH_{a(1)}$ into Eq. (3.4) and using the current value of $F_{A(O_2)}$, we obtain $C_{a(HbO_2)(1)}$ from Eq. (3.3). Then using $C_{a(HbO_2)}$, we solve Eq. (3.1) for $C_{a(CO_2)(2)}$. We do this by a process of iterative guessing, putting $C_{a(CO_2)(1)}$ on the right hand side, calculating $C_{a(CO_2)(2)}$ on the left, comparing the two, adjusting $C_{a(CO_2)(1)}$ and repeating until the two agree within a predetermined limit of error. Now, using this new value for $C_{a(CO_2)}$, we repeat the entire process, recalculating pH_a, $C_{a(HbO_2)}$, and $C_{a(CO_2)}$ until we get a $C_{a(CO_2)}$ that satisfies Eq. (3.1) on the first trial. Going next to the brain, we solve Eq. (4.1) for $P_{B(CO_2)}$, using the current value of $C_{B(CO_2)}$. Again we use an iterative guessing procedure, but since HbO_2 is not involved here, it is unnecessary to include the pH and HbO_2 steps. Then using this value of $P_{B(CO_2)}$, the current value of $C_{B(O_2)}$, and an initial trial guess for $C_{vB(CO_2)}$, we apply the complete iterative procedure to Eqs. (4.2)-(4.7) to obtain current values for $C_{vB(CO_2)}$, $C_{vB(O_2)}$ and pH_{vB}. Finally, going to the tissue reservoir, we apply

the same technique to Eqs. (5.1)-(5.7) to obtain current values for $P_{T(CO_2)}$, $C_{vT(CO_2)}$, $C_{vT(O_2)}$, and pH_{vT}.

A second feature involves the storage and retrieval of the "lag variables" defined by Eqs. (8.1)-(8.9). Provision is made for storing in the computer previous values of these variables in a table, continuously updated, that extends an appropriate distance into the past, usually 0.5-1.5 minutes. After calculating current values for the lag times, an interpolation routine is used to retrieve the proper values of the lag variables for use in the next integration step. In early versions of the program, current rather than average blood flow values were used to calculate the required τ values, but in later versions, the correct average values were computed. To obtain these it was necessary to integrate the various blood flow-time functions "backwards" into the past, starting at current time and stopping when the value of the integral became equal to the appropriate vascular volume. This point defined the lower limit of the integration and hence the appropriate τ.

Finally, for convenience in future explorations and modifications, the programs have been written in the form of multiple subroutines, each of which can be altered more or less independently of the others. The latest version of our Fortran IV program includes approximately 500 statements.* A sample tabular output is provided in App. C, and graphs of the material will be discussed below.

5. RESULTS

The equations of the model and the corresponding digital simulations have evolved through several stages cf increasing complexity. In the first version there was no CSF compartment, and values were

---

*Programs are available from the authors on request.

computed from current rather than "past-average" blood flows. The controller inputs were brain P_{CO_2}, brain (H^+), and arterial P_{O_2} at the peripheral chemoceptors. A variety of forcings were studied including: (a) CO_2 inhalation (1, 3, 5 percent) and recovery; (b) hypoxia at sea level (10, 8, 6 percent O_2) and recovery; and (c) altitude hypoxia (15,000, 18,000, 20,000 feet). With few exceptions, the solutions were stable, and the quasi-steady state values were close to those expected in the prototype (Table 1). It is noteworthy that a true steady state, if judged by the alveolar RQ calculated at each step, was not attained in 30 minutes for any of the forcings except perhaps 1 percent CO_2. Transient behavior during CO_2 inhalation and recovery was similar in form to that of an earlier model [3]; an example is given in Fig. 2. However, it will be noted that the "on response" of ventilation is much faster in the present
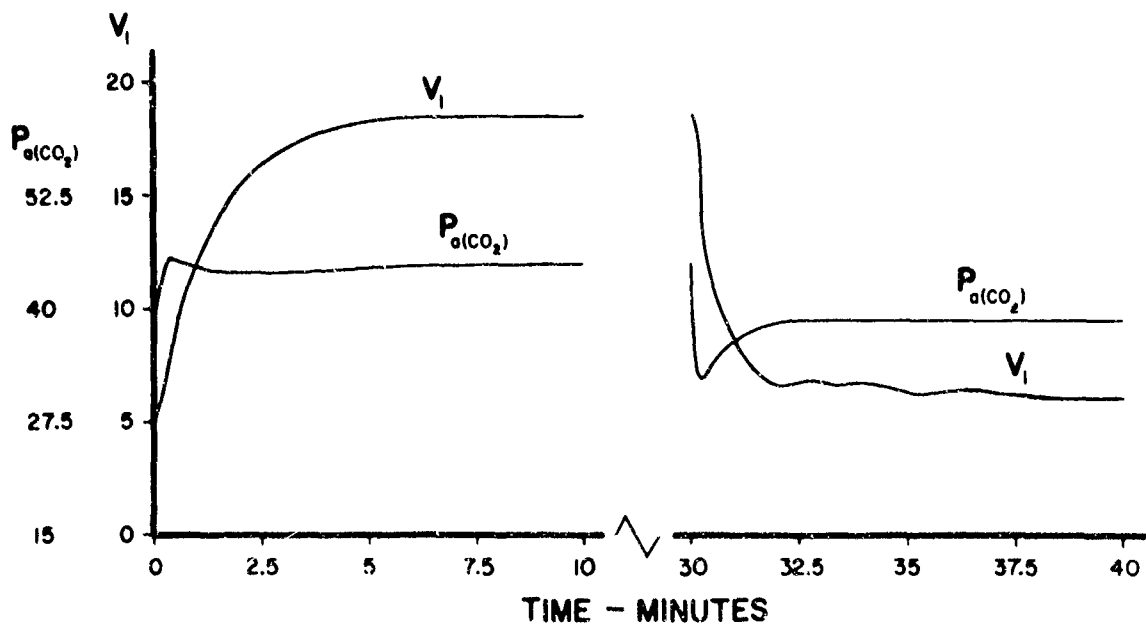
Fig. 2—Response of Version 1 to 5% CO_2 "pulse."
Pulse on at zero time, off at 30 min.

Table 1

Table 1

STEADY STATE VALUES—VERSION 1

Variable*	Normal Control	CO_2 Inhalation			Hypoxia at Sea Level			Hypoxia at Altitude		
		1% CO_2	3% CO_2	5% CO_2	10% O_2	8% O_2	6% O_2	15,000'	18,000'	20,000'
V_I	5.07	6.10	9.88	16.67	6.44	10.36	11.09	5.73	6.48	7.12
V_E	5.03	6.06	9.84	16.61	6.42	10.33	11.12	5.67	6.44	7.09
$F_A(CO_2)$	.0557	.0563	.0585	.0665	.0473	.0405	.0316	.0948	.0994	.1020
$F_A(O_2)$	.1480	.1585	.1783	.1913	.0505	.0405	.0311	.1069	.1052	.6945
$F_A(N_2)$	.7963	.7852	.7632	.7422	.9021	.9190	.9372	.7982	.7954	.7933
$P_A(CO_2)$	39.7	40.1	41.7	47.4	33.7	28.9	22.6	36.2	33.1	30.8
$P_B(CO_2)$	50.2	50.7	52.6	55.9	40.0	34.8	26.2	43.0	39.2	36.4
$P_T(CO_2)$	44.7	45.1	46.4	51.4	37.1	31.7	25.1	39.7	36.3	33.8
$P_A(O_2)$	105.5	113.0	127.1	136.4	36.0	28.9	22.2	40.8	35.0	31.6
$P_B(O_2)$	37.3	37.8	38.7	48.1	24.2	21.5	16.1	27.0	23.6	21.6
$P_T(O_2)$	47.2	48.0	51.2	58.5	28.2	23.4	18.3	31.1	27.5	25.3
$C_a(CO_2)$	.5748	.5768	.5846	.6118	.5551	.5285	.4857	.5672	.5517	.5393
$C_B(CO_2)$	.6415	.6435	.6513	.6597	.6081	.5710	.5230	.6148	.5980	.5842
$C_T(CO_2)$	.6094	.6111	.6160	.6363	.5816	.5532	.5112	.5939	.5773	.5643
$C_a(HbO_2)$	.1976	.1983	.1991	.1993	.1430	.1262	.1080	.1525	.1409	.1332
$C_{vB}(HbO_2)$	.1331	.1340	.1352	.1542	.0970	.0835	.0781	.1055	.0952	.0890

Table 1—continued

Variable*	Normal Control	CO₂ Inhalation			Hypoxia at Sea Level			Hypoxia at Altitude		
		$1\% CO_2$	$3\% CO_2$	$5\% CO_2$	$10\% O_2$	$8\% O_2$	$6\% O_2$	15,000'	18,000'	20,000'
$C_{vT}(HbO_2)$	.1585	.1598	.1642	.1718	.1147	.1012	.0848	.1222	.1130	.1067
$C_B(O_2)$	.0012	.0012	.0012	.0015	.0008	.0007	.0005	.0008	.0007	.0007
$C_T(O_2)$	.0015	.0015	.0016	.0018	.0009	.0007	.0006	.0010	.0009	.0008
$C_B(N_2)$	.0097	.0096	.0093	.0091	.0110	.0012	.0115	.0052	.0045	.0041
$C_T(N_2)$	.0097	.0096	.0093	.0091	.0110	.0112	.0114	.0052	.0045	.0041
pH_a	7.411	7.408	7.397	7.359	7.469	7.517	7.590	7.447	7.476	7.500
pH_B	7.354	7.350	7.340	7.318	7.429	7.468	7.556	7.406	7.435	7.458
pH_T	7.384	7.381	7.372	7.340	7.447	7.500	7.566	7.426	7.454	7.382
Q	6.00	6.04	6.52	8.22	8.60	9.51	10.59	8.08	8.72	9.15
Q_B	.750	.750	.750	1.04	1.08	1.17	1.37	1.05	1.08	1.12
Alveolar RQ	.875	.874	.872	.848	.952	1.02	1.10	.901	.935	.960
Time	•	30	30	30	30	30	30	30	30	30	30

*See App. A for definition of symbols.

model, requiring only 3 minutes to reach the 80 percent level rather than the 12 minutes needed by the original version [3]. This difference has also been noted by others [5, 9] who have separated out a brain compartment from the single lumped tissue reservoir previously assumed [3]; it is directly related to the relative ratios of compartment volume to blood flow. Closer attention to the early details of the prototype response [19-21] has indicated that neither model is too faithful, for there appears to be an initial fast response of relatively modest magnitude followed by a much slower but larger component. Moreover, the ventilatory response lags considerably behind the change in jugular venous P_{CO_2} after the first minute [19]. These matters will be referred to again later. As expected, a short interval of periodic breathing occurred on sudden return to air after a prolonged period of hypoxia (Fig. 3). Figure 4 shows a phenomenon occasionally encountered, i.e., the sudden appearance of numerical instability in a previously stable solution in this case after 35 minutes at an altitude of 20,000 feet. Disappearance of this behavior on changing the integration step size confirms the suspicion that it is a computational and not a model instability.*

In the second stage of development, a CSF reservoir was added, but τ values were still computed from current blood flows. The controller inputs were now the CSF (H^+), and both arterial (H^+) and

---

*With single precision arithmetic, a step size of 0.01 minute was satisfactory on the CDC 3400 (48-bit word). On the IBM 7044 (36-bit word), a step size of 0.007812, i.e., $1/2^7$, was usually satisfactory, but occasionally a smaller one was required ($1/2^8$ or $1/2^9$).
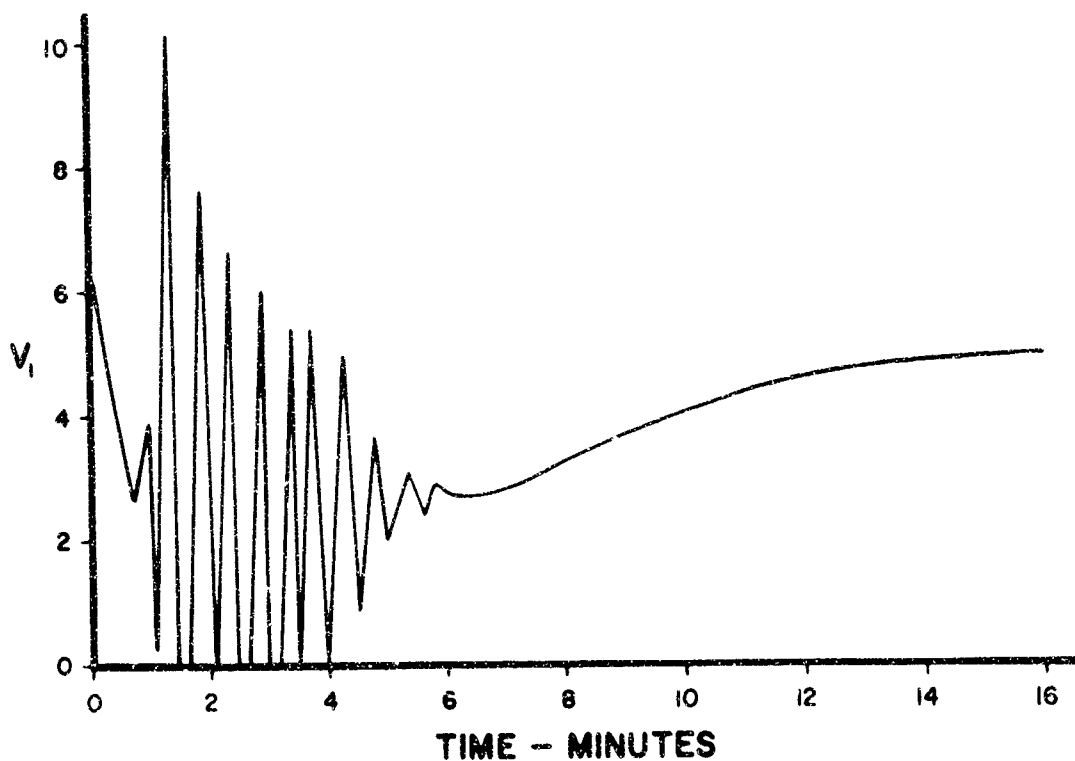
Fig. 3—Periodic breathing on recovery from hypoxia (30 min on 10% O_2, Version 1). Value $F_{I(O_2)}$ changed exponentially from 0.10 to 0.21 during first min.
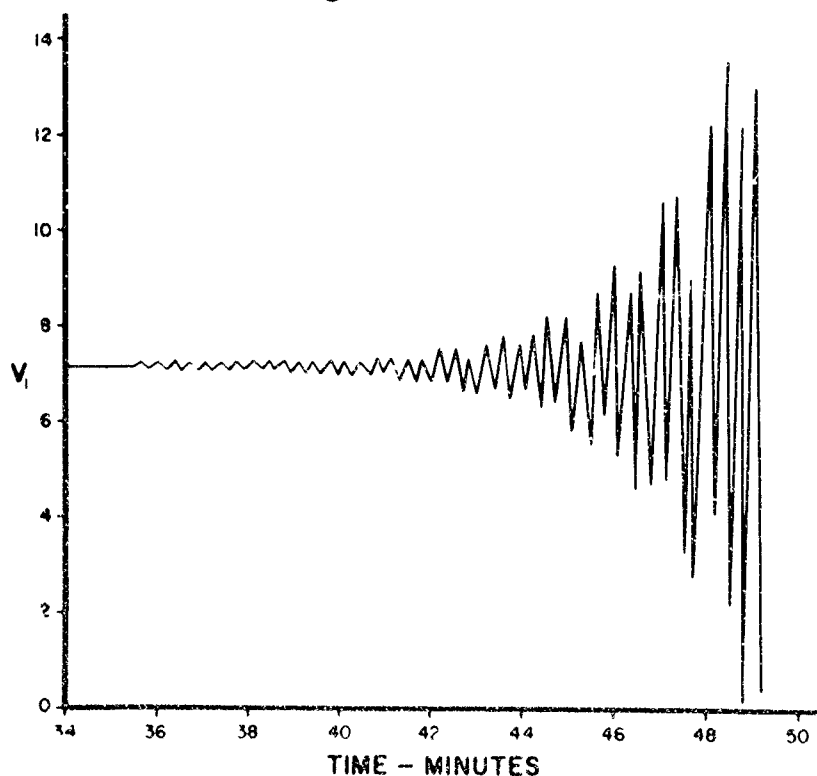
Fig. 4—Sudden appearance of numerical instability after 35 min at 20,000 ft. Version 1.

P_{O_2} at the peripheral chemoceptors, a control scheme similar to that suggested by Lambertsen [19], and compatible with the recent work of Mitchell, et al. [18]. This control function should introduce both fast and slow components into the CO_2 response, and should also permit a preliminary study of responses to metabolic acidosis. Figure 5 shows the behavior of ventilation, CSF (H^+), and arterial (lung exit) (H^+) during and following a 30 minute "pulse" of 5 percent CO_2 in inspired air. The similarity of the "on transient" to the behavior observed in dogs by Lambertsen [19] is apparent. In contrast with Version 1, ventilation once more requires 12 minutes to reach 80 percent of its total response, but in contrast with our original
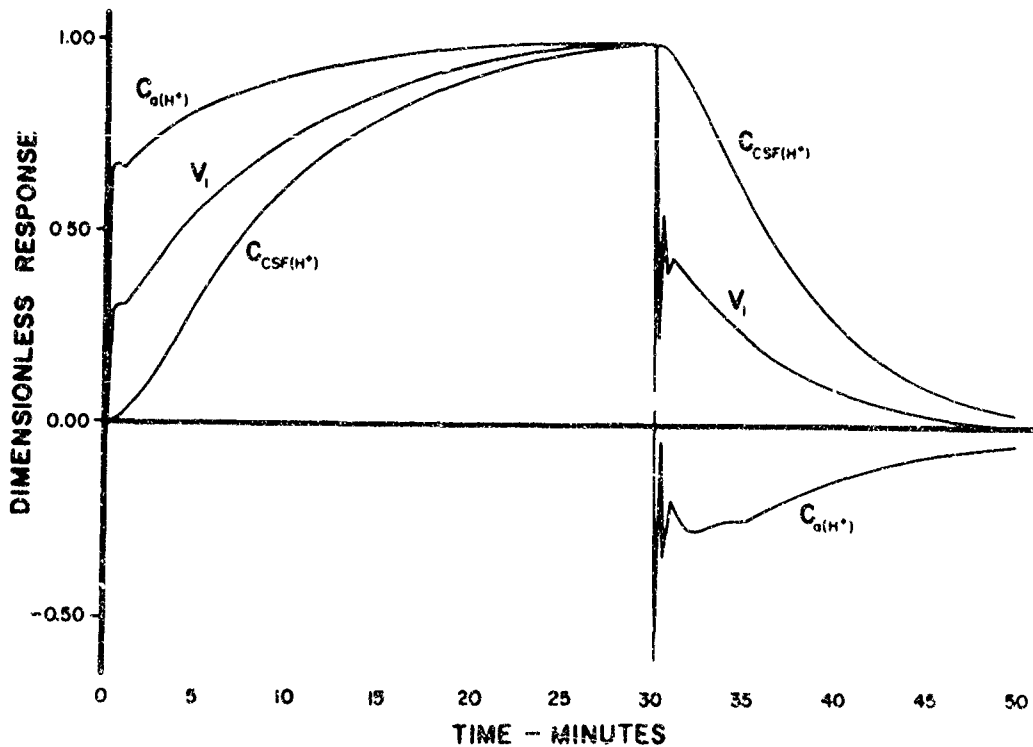
Fig. 2—Response of Version 1 to 5% CO_2 "pulse."
Pulse on at zero time, off at 30 min.

model [3] and in agreement with recent observations [19-21], we now
also have an initial rapid component so that about 30 percent of
the response occurs within one minute. The exact relationship
between the three curves in Fig. 5 can be altered by changing the
relative weightings assigned to peripheral and CSF (H^+) receptors.
Although the entire time course of the response to metabolic acidosis
was obtained, the transient portion is not really very relevant, for
the forcing was introduced in a highly artificial manner, i.e.,
a step change in $(BHCO_3)_b$ and $(BHCO_3)_T$ at zero time while keeping
$(BHCO_3)_B$ and $(BHCO_3)_{CSF}$ constant. However, it is of interest that
a stable solution was obtained and that the steady state values
shown in Table 2 are quite realistic [2]. Thus, the same reduction
in arterial pH produced by 5 percent CO_2 inhalation on the one hand,
and by metabolic acidosis on the other was associated with a ventila-
tion ratio of 3.66 in the former and only 1.25 in the latter. Whereas
CO_2 inhalation produced hypercapnia and increased (H^+) throughout
the body, the increase in (H^+) in metabolic acidosis was confined
to the blood and "not-brain" tissue, while the (H^+) of brain and
CSF actually fell. Thus the general qualitative and quantitative
behavior of the model seems quite reasonable under these conditions.

The major modification introduced into the third version of the
model was the use of correct "past-average" blood flow values to
compute current values for the time lags. This did not produce any
significant difference in the response to a 5 percent CO_2 pulse.
The computer generated graph of Fig. 6 includes the time course of
brain (or internal jugular) (H^+) which is identical with that of
brain P_{CO_2} on this non-dimensional plot, and this leads the ventila-
tory response after the first minute of the "on" transient, in
agreement with experimental observations noted previously [25].

Table 2

STEADY STATE VALUES—VERSION 2

Variable*	Normal Control	Metabolic Acidosis	5% CO_2
V_I	5.37	6.71	19.66
V_E	5.33	6.67	19.62
$F_{A(CO_2)}$	.0526	.0421	.0644
$F_{A(O_2)}$	.1514	.1632	.1941
$F_{A(N_2)}$	.7959	.7947	.7415
$P_{A(CO_2)}$	37.5	30.0	45.9
$P_{B(CO_2)}$	47.8	43.4	55.3
$P_{CSF(CO_2)}$	47.8	43.4	55.2
$P_{T(CO_2)}$	42.3	34.5	50.1
$P_{A(O_2)}$	108.0	116.3	138.4
$P_{B(O_2)}$	36.5	32.4	45.0
$P_{CSF(O_2)}$	36.2	32.1	44.6
$P_{T(O_2)}$	46.7	50.6	57.0
$C_{a(CO_2)}$	.5629	.3966	.6048
$C_{B(CO_2)}$	.6396	.6185	.6718
$C_{CSF(CO_2)}$	.6172	.6142	.6222
$C_{vB(CO_2)}$	.6309	.4855	.6588
$C_{T(CO_2)}$	.6130	.4212	.6500
$C_{vT(CO_2)}$	.5975	.4300	.6314
$C_{a(HbO_2)}$	.1981	.1982	.1994
$C_{vB(HbO_2)}$	.1324	.1120	.1483
$C_{vT(HbO_2)}$	.1592	.1608	.1705
pH_a	7.427	7.370	7.368
pH_B	7.375	7.404	7.331

Table 2—continued

Variable*	Normal Control	Metabolic Acidosis	5% CO_2
pH_{CSF}	7.344	7.386	7.281
pH_{VB}	7.369	7.293	7.322
pH_T	7.412	7.334	7.361
pH_{VT}	7.401	7.344	7.348
Q	6.00	6.00	7.77
Q_B	.736	.562	.926
Alveolar RQ	.875	.875	.874
Time	∞	77	49

*See App. A for definition of symbols.
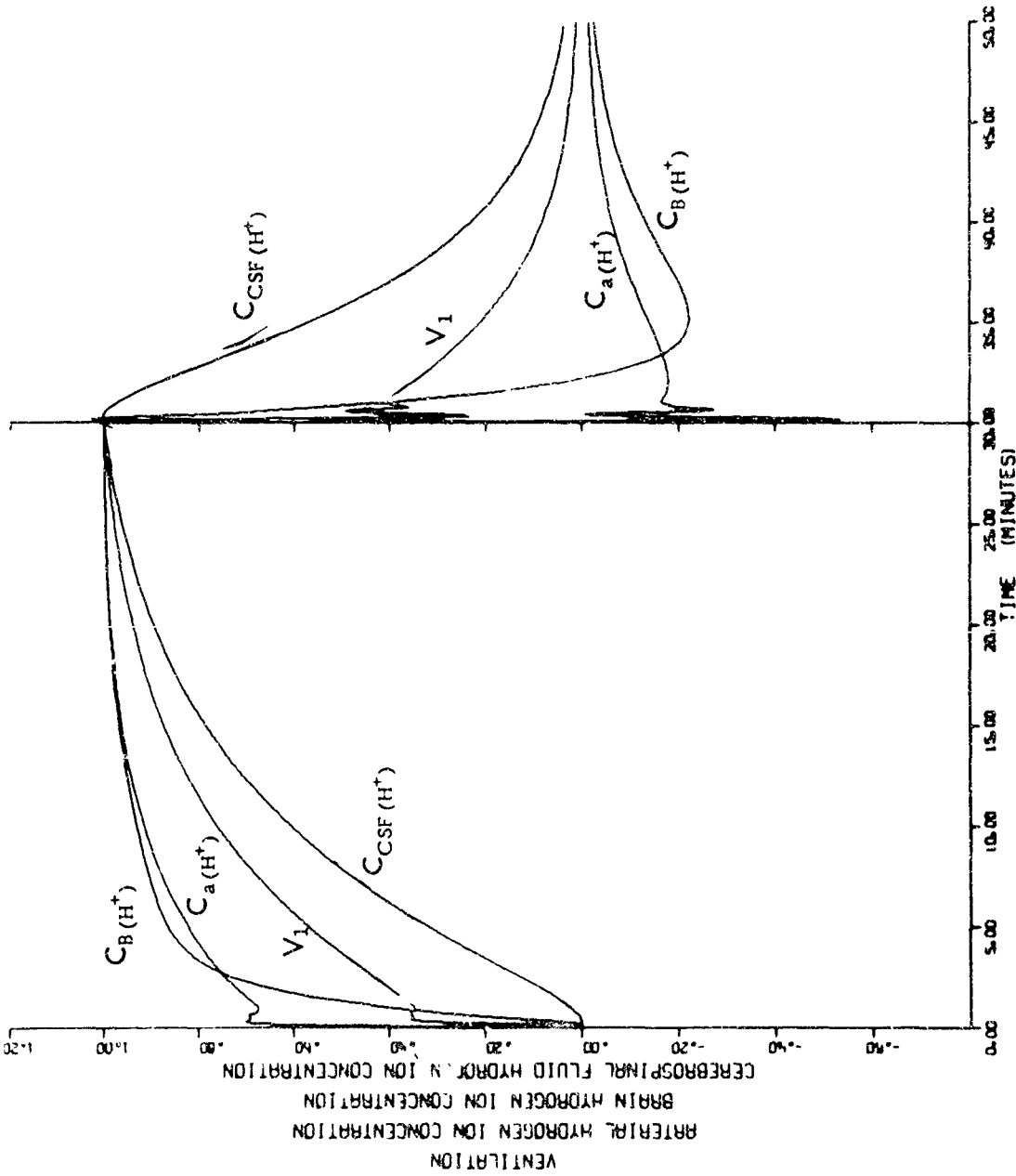
Fig. 6—Computer generated plot of Version 3 response to 5% CO_2 pulse. Pulse on at zero time, off at 30 min. Non-dimensional ordinate scale.

Early details of the "on" and "off" transients appear in the expanded
time scale graphs of Fig. 7. The response to a 30 minute "pulse" of
10 percent oxygen with subsequent return to air is shown in Figs. 8–10.
Prominent features are the ventilation overshoot during the "on"
transient (Fig. 8), and the prolonged interval of periodic breathing
during recovery (Fig. 10). This periodicity persists longer than it
did in Version 1 (Fig. 3), but in the latter, return to air was accom-
plished gradually over one minute whereas in the present example
it was instantaneous. Also nicely illustrated is the sequence:
$P_{A(O_2)}$ fall–delay–ventilation rise–$P_{A(CO_2)}$ and $C_{a(H^+)}$ fall at the
start of hypoxia (Fig. 8), as well as the sequence: $P_{A(O_2)}$ rise–
delay–ventilation fall–$P_{A(CO_2)}$ and $C_{a(H^+)}$ rise at the start of
recovery (Fig. 9).

6. DISCUSSION

A major purpose of the present study was to provide a suf-
ficiently detailed mathematical description and digital simulation
of the "plant" so that a significantly wide variety of forcings
and control hypotheses could be explored. This has been accomplished
to some extent, the plant description taking the form of a set of
differential–difference equations, incorporating a number of dependent
time–delays, which express the basic material balance relationships
of the system. Additional equations are required to define the
chemical details of gas transport and acid–base buffering mechanisms,
concentration equilibria in various parts of the system, and the
dependence of blood flow rates upon CO_2 and O_2 concentrations.
Finally, a control loop manipulating pulmonary ventilation according
to any one of a variety of possible schemes can be included. The
model is sufficiently general to accept many sorts of forcings, e.g.,
CO_2 inhalation, hypoxia at sea level or at altitude, metabolic
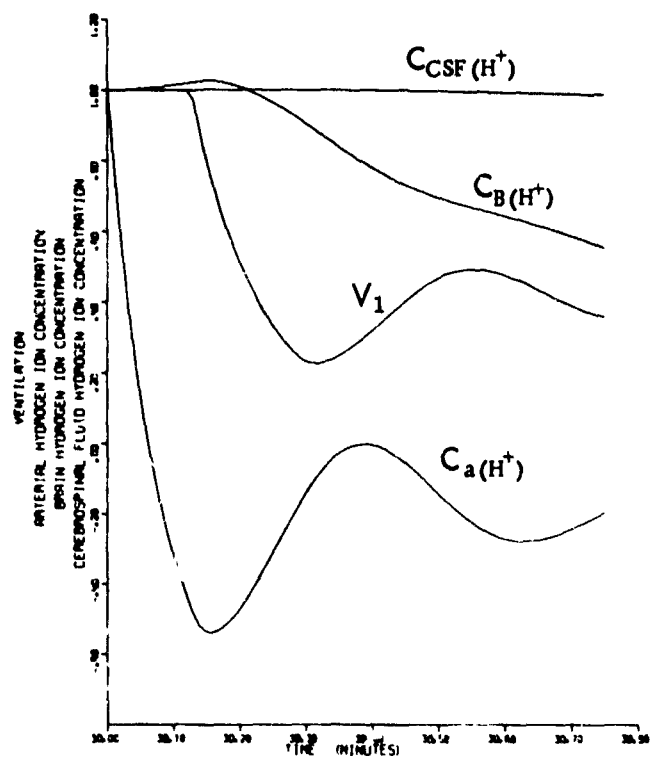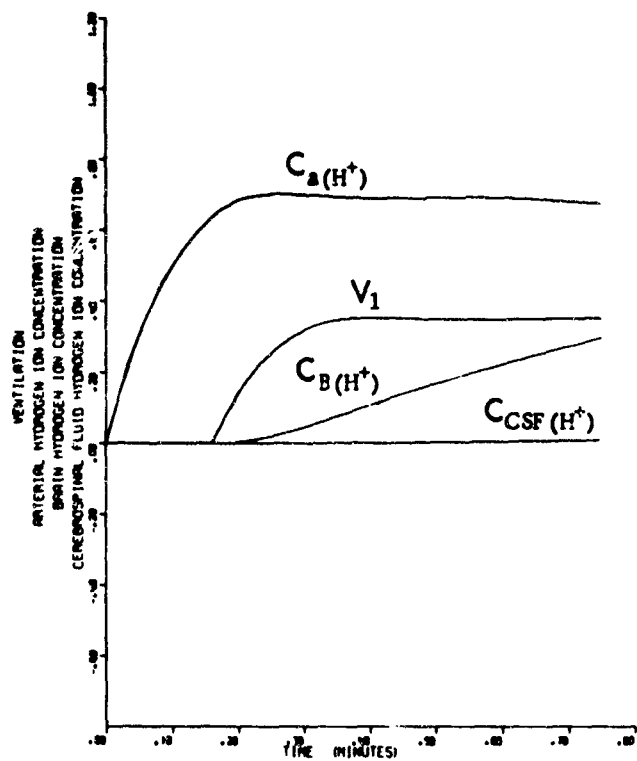
Fig. 7—Expanded time scale plots of Fig. 6
for intervals 0.00–0.75 min and 30.00–30.75 min to show early
details of on and off transients.
Non–dimensional ordinate scales.
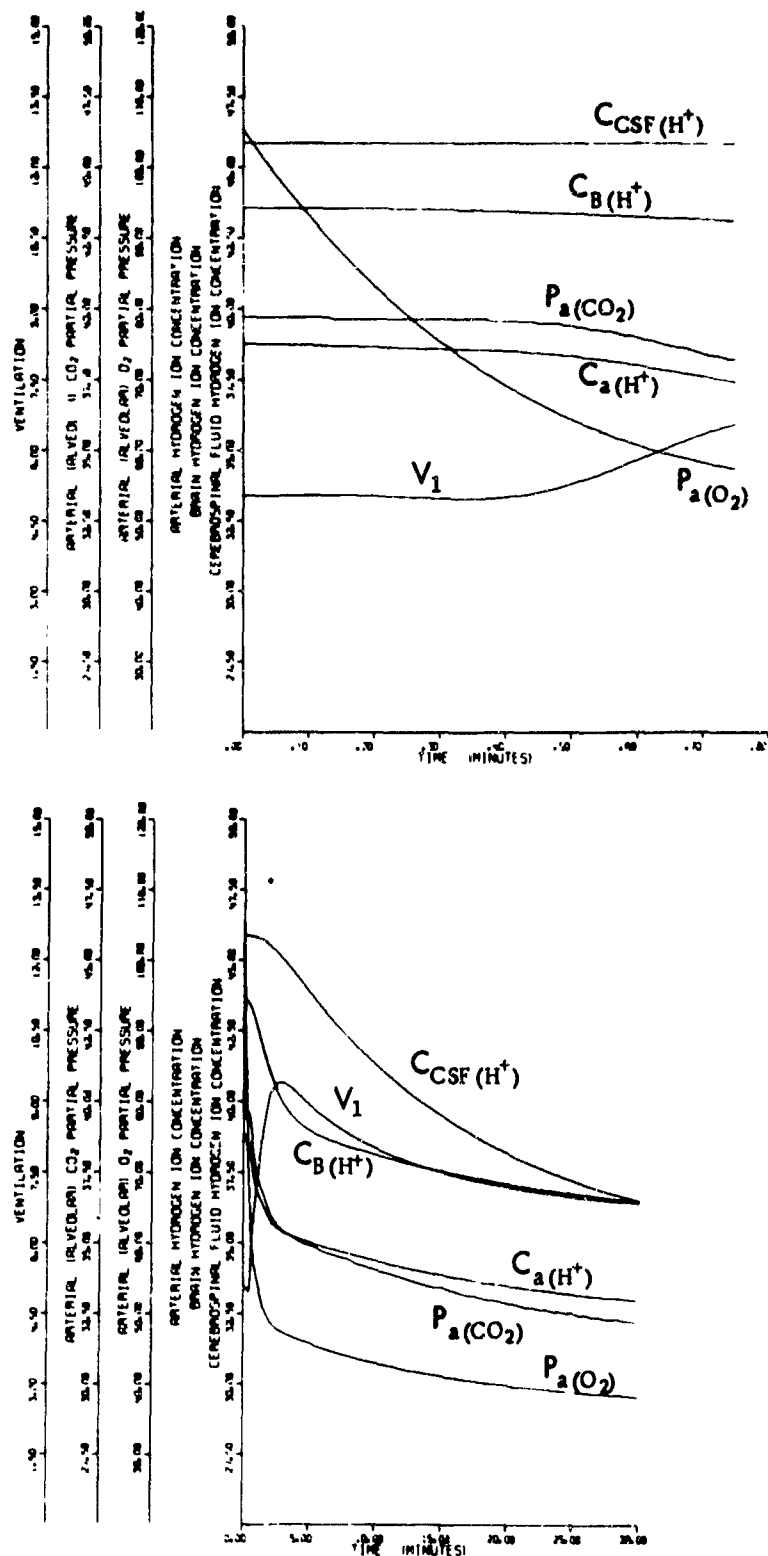
Fig. 8—Computer plots of response of Version 3
to step input of 10% O_2.
Expanded time scale plot above shows early detail.
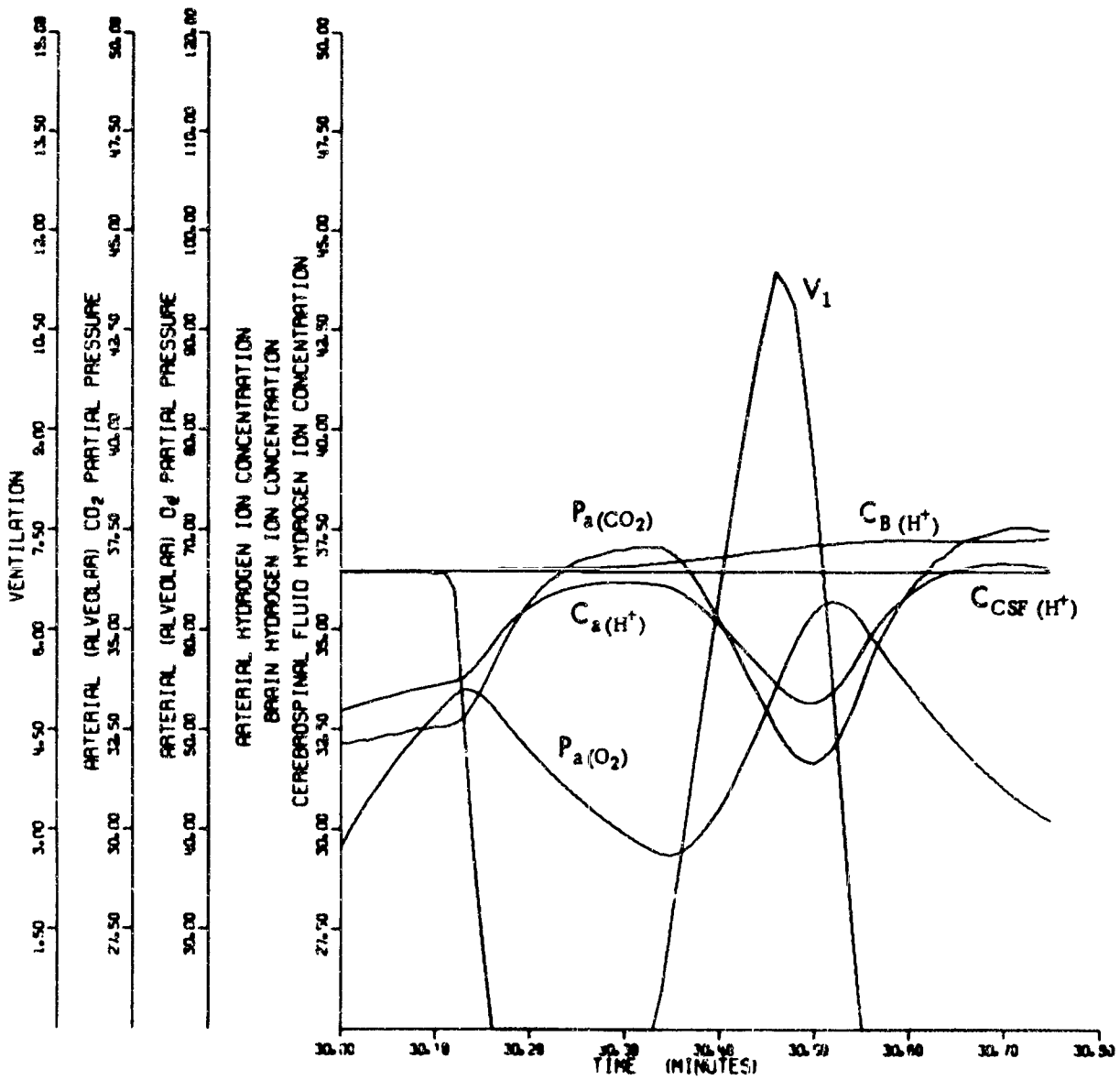
Fig. 9—Computer plot of behavior of Version 3
during first 0.75 min following instantaneous return to
air after 30 min on 10% O_2.
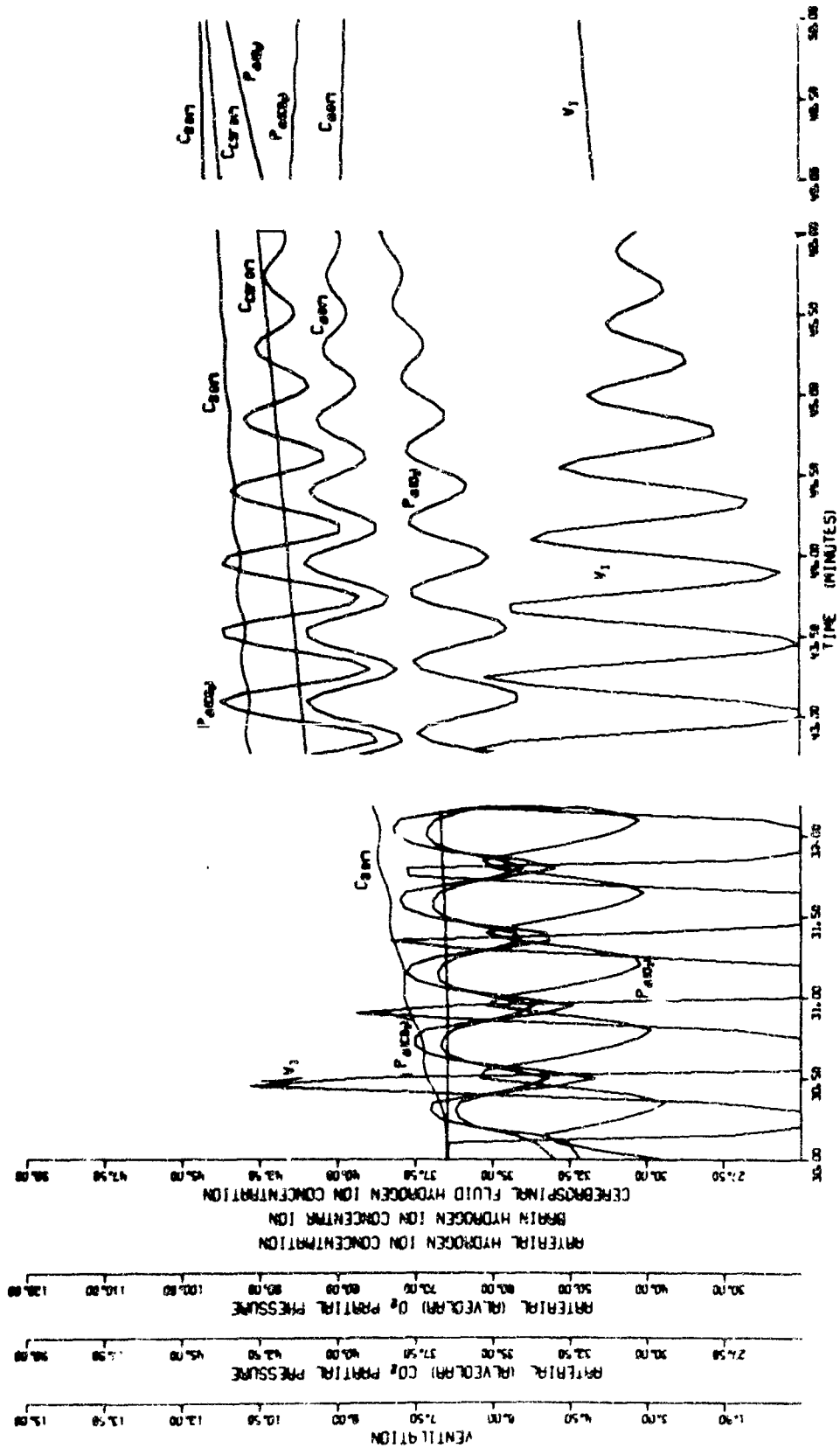
Fig. 10—Continuation of Fig. 9 with compressed time scale to show subsequent course of recovery from hypoxia.

acidosis and alkalosis, or any combinations thereof, and any arbitrary
time course can be assigned to them. Concentrations of a variety
of chemical species are available at several different locations
for use in possible control functions. Extension of the model to
include any number of additional distinct tissue compartments is
simple in principle, as in the inclusion of other inhaled agents
such as anesthetics.

Solution of this system of nonlinear equations would be completely
impractical without computer assistance. The digital computer is
particularly suited for large multivariate systems incorporating
time delays, although the storage requirements for retaining the past
histories of many variables may get uncomfortably large. To our
knowledge, this is the first time that a set of differential—difference
equations whose time delays themselves are dependent variables has
been solved by digital techniques [22]. The latest version of our
program requires about one minute of machine time (CDC 3400) for
every four minutes of experimental simulation.

Indicative of the importance of dynamic simulation is the fact
that many recent contributions to our understanding of the "chemical
control" of ventilation have been based upon the study of dynamic
transients in an attempt to separate peripheral (fast) from central
(slow) components [19—21]. Such studies led Lambertsen [19] to
suggest a dual sensing mechanism for the ventilatory response to
CO_2, one receptor responding directly to arterial (H^+) and the other
to the (H^+) of an appropriate central fluid, perhaps CSF. This
suggestion fits in very well with the results of Dejours' "two breath
CO_2 test" before and after chemoceptor denervation [20, 21] as well
as with other observations indicating the existence of superficial
medullary receptors sensitive to CSF (H^+) [18]. A control scheme

of this sort incorporated into our model closely reproduced Lambertsen's observations. In both experiment and model (Fig. 6), arterial P_{CO_2} (or (H^+)) changed most rapidly, followed in order by brain venous P_{CO_2} (or (H^+)), ventilation, and finally CSF P_{CO_2} (or (H^+)). It is not essential to this scheme that the central receptors be superficial and exposed directly to "bulk CSF," for they could lie somewhat deeper within the medulla in accordance with the classical view and the recent studies of Pappenheimer, et al. [25], responding to the (H^+) of the appropriate local central fluid. It is essential, however, that there be a separate arterial receptor for (H^+) else the results of chemoceptor denervation could not be accounted for [20, 21].

Dejours [20], and Bouverot, et al. [21], have also used a "two breath O_2 test" to study the peripheral (fast) response to 100 percent O_2. They noted the difficulty of assessing the mechanism of the ventilatory response to long lasting pure oxygen inhalation because of the operation of many other factors involving the gas transport systems Such factors are taken into account in the present model, and prolonged administration of 100 percent O_2 in Version 1 resulted in a mild hyperventilation associated with arterial hypocapnia and alkalemia together with brain and venous hypercapnia and increased (H^+) [26]. The initial depression of ventilation observed by Dejours was not reproduced, for we have not yet rewritten our control function to include an "O_2 threshold" as high as 200 mm Hg. We are confident that this modification together with an appropriate interaction term involving arterial (H^+) and P_{O_2} at the carotid chemoceptors will permit Version 3 of our model to reproduce Dejours' CO_2 and O_2 results in detail.

Although step or pulse inputs of gases are convenient and widely used forcings, the production of metabolic disturbances in acid-base balance is carried out in a variety of nonstandard ways ranging from intravenous injection of acid or alkali to prolonged ingestion of NH_4Cl or $NaHCO_3$ or diabetic accumulation of ketone bodies. The nature of the transient response is of course critically dependent upon the time course of the forcing function, and while it is possible to simulate a wide variety of these in the model, we have not yet carried out any such systematic exploration. Very recently, the primary role of the peripheral chemoceptors in the ventilatory responses to metabolic acid-base disturbances as conceived by Mitchell, et al. [27], has been questioned by Fencl, Miller, and Pappenheimer [28], who found changes in CSF (H^+) deemed sufficient to account for the behavior of ventilation. There also seems to be disagreement as to whether chemoceptor denervation abolishes ventilatory responses to metabolic acid-base disturbances [29, 30]. Although some of this disagreement may be more apparent than real and dependent upon such factors as the severity and duration of the disturbance, presence or absence of anesthesia, species difference, etc., it is apparent that much more work is needed here to define the details of material transport and buffering mechanisms in the brain as well as the location of the central chemoceptors.

Despite some obvious defects, the present model thus seems to provide a useful dynamic summary and synthesis of much of our present understanding of lung-blood-tissue gas transport, acid-base buffering, and what is generally called the "chemical control of pulmonary ventilation." Although many of its features can also be found in other recent models [5-9], the present version is perhaps somewhat more complete and general. It can serve as a convenient base for

studying sensitivity to parameter variations, for exploring modified
control modes, and for gradual expansion to include aspects so far
neglected. With this in mind, the digital simulation program has
been made flexible enough to allow convenient modification and
expansion.

That both modification and expansion will be necessary is
abundantly clear: Our treatment of tissue buffering and material
exchange across the blood—brain barrier is at best only a very crude
first approximation. As noted above, detailed knowledge of these
matters is both important and lacking. The model does not account
for the hyperpnea of exercise, and although we could easily introduce
a term proportional to O_2 consumption into our control function to
accomplish this [31], the "physiological isomorphism" of such a term
still seems to be obscure [32]. Moreover, attempting to account for
exercise hyperpnea in this way would make it painfully obvious that
the model includes no really general description of the control of
cardiac output and regional blood flow. Since the respiratory and
cardiovascular systems are really part of a single gas transport
system, close coupling between their control mechanisms might be
expected, and it would seem that a real understanding of either
requires an understanding of both [33].

Coupling between various physiological systems treated as a
collection of nonlinear oscillators has been considered by Iberall
and Cardon [34], and spectral analyses of skin temperature [34] and
ventilation [34, 35] time series obtained from normal resting men
have been carried out in efforts to identify significant frequencies.
Four major periods appear, which Iberall suggests may be associated
with a metabolic rate cycle (1-2 minutes), a vasomotor cycle (5-10
minutes), a tissue gas storage cycle (20-40 minutes), and a tissue
heat storage cycle (2 hours). Our model includes tissue gas storages

with relatively long time constants, short lags in the response of
cardiac output and brain blood flow, and a number of short blood
transport delays. The latter are primarily responsible for the short
period oscillations (about 0.5 minute) observed in the model during
the early stages of recovery from hypoxia or CO_2 inhalation. It is
certainly possible that tissue metabolic rate is normally periodic
at rest as suggested by Iberall, and it is well known that capillary
blood flow, at least in some vascular beds, is intermittent [36],
but we have not yet included these possibilities in our model.

Finally, although the "chemorespiratory" physiologist interested
primarily in the physics, chemistry, and control of lung-blood-tissue
gas transport, buffering and exchange might be reasonably happy with
this model, the "neurorespiratory" physiologist interested primarily
in the intimate central neural mechanism of respiratory cycle genera-
tion will not be happy with it at all. Certainly there are no illumina-
ting insights here for him! Perhaps this points out the most fruitful
direction for further work both experimental and theoretical, providing
we remember that "neural control" and "chemical control" are not
mutually exclusive but are interrelated parts of a single mechanism.

Appendix A

SYMBOLS AND UNITS FOR EQUATIONS OF SYSTEM

A.1. EXPLANATION

A complete symbol has the general form, $A_{i,j}$, where A designates the class of variable (e.g., solubility coefficient, concentration, metabolic rate, etc.), i specifies the location (e.g., brain, blood at lung exit, etc.), and j identifies the chemical species (e.g., O_2, CO_2, H^+, etc.). In certain cases, one or both subscripts are omitted (e.g., Q $\equiv$ cardiac output; B $\equiv$ barometric pressure).

A.2. TABLE OF SYMBOLS AND UNITS

Character	Subscripts		Definition	Units
	Location (i)	Species (j)		
α			solubility coefficient	
		·gas	for gas in blood	liter (STPD)/liter blood/atm, 37°C
	B	(gas)	for gas in brain	liter (STPD)/liter brain/atm, 37°C
	T	(gas)	for gas in tissue	liters (STPD)/liter tissue/atm, 37°C
	CSF	(gas)	for gas in cerebro-spinal fluid	liters (STPD)/liter CSF/atm, 37°C
B			barometric pressure	mm Hg
(BHCO₃)			standard bicarbonate content	
	b		of blood	liters CO_2(STPD)/ liter blood, 37°C
	B		of brain	liters CO_2(STPD)/ liter brain, 37°C
	T		of tissue	liters CO_2(STPD)/ liter tissue, 37°C

| Char-acter | Subscripts | | Definition | Units |
	Loca-tion (i)	Species (j)		
	CSF		of cerebrospinal fluid	liters CO_2(STPD)/ liter CSF, $37^\circ C$
C			concentration	
		(gas)	of gas	liters (STPD)
		(HbO_2)	of oxyhemoglobin	liters O_2(STPD)
		(H^+)	of hydrogen ion	nanomoles
	a		in blood at lung exit	liter blood^{-1}
	aB		in blood at brain entrance	liter blood^{-1}
	aT		in blood at tissue entrance	liter blood^{-1}
	B		in brain	liter brain^{-1}
	CSF		in cerebrospinal fluid	liter CSF^{-1}
	T		in tissue	liter tissue^{-1}
	v		in blood at lung entrance	liter blood^{-1}
	ao		in blood at carotid body	liter blood^{-1}
	vB		in blood at brain exit	liter blood^{-1}
	vT		in blood at tissue exit	liter blood^{-1}
D		gas	diffusion coefficient for gas across "blood-brain" barrier	liters (STPD)/min/ mm Hg
F			volumetric fraction	dimensionless
		(gas)	of gas	
	A		in dry alveolar gas	
	E		in dry expired gas	
	I		in dry inspired gas	
(Hb			blood oxygen capacity	liters (STPD)/liter blood
`			conversion factor	atm/mm Hg
K'			dissociation constant	
			for carbonic acid	nanomoles/liter
K			ume	liters
	B		o brain	
	CSF		cerebrospinal fluid	

Character	Subscripts Location (i)	Subscripts Species (j)	Definition	Units
	T		of tissue	
	L		of alveoli	
MR			metabolic rate	liters (STPD)/min
		(CO_2)	of carbon dioxide production	
		(O_2)	of oxygen consumption	
	B		by brain	
	T		by tissue	
P			tension or partial pressure	mm Hg
		(gas)	of gas	
	A		in alveoli	
	a		in blood at lung exit	
	B		in brain	
	CSF		in cerebrospinal fluid	
	I		in inspired air	
pH			pH	
	a		of blood at lung exit	
	vB		of blood at brain exit	
	vT		of blood at tissue ex'	
	CSF		of cerebrospinal fluid	
Q			blood flow	liters/min
			cardiac output	
	B		cerebral	
	N		normal (resting)	
ΔQ			change in blood flow	liters/min
	—		cardiac output	
	B		cerebral	
		(CO_2)	due to carbon dioxide	
		(O_2)	due to oxygen	
r			time constant	minutes
	1		for cardiac output response	
	2		for cerebral blood flow response	
t			time	minutes

Char-acter	Subscripts		Definition	Units
	Loca-tion (i)	Species (j)		
τ			blood transport delay	minutes
	aB		from lung to brain	
	aT		from lung to tissue	
	vB		from brain to lung	
	vT		from tissue to lung	
	ao		from lung to carotid body	
		(1)	in appropriate segment of total path	
V	i		gas flow rate (alveolar)	liters (BTPS)/min
	E		expiratory	
	I		inspiratory (i.e., ventilation)	

Appendix B

"NORMAL" PARAMETER VALUES[*]

α_{CO_2}	=	0.510[**]	k	=	0.00132
α_{O_2}	=	0.0240	K'	=	795
α_{N_2}	=	0.0130	K_B	=	1.000
B	=	760	K_{CSF}	=	0.100
$(BHCO_3)_b$	=	0.5470	K_T	=	39.00
$(BHCO_3)_B$	=	0.5850[***]	K_L	=	3.00
$(BHCO_3)_T$	=	0.5850[***]	$MR_{B(CO_2)}$	=	0.050
$(BHCO_3)_{CSF}$	=	0.5850	$MR_{B(O_2)}$	=	0.050
D_{CO_2}	=	81.99×10^{-7}	$MR_{T(CO_2)}$	=	0.182
D_{O_2}	=	4.361×10^{-7}	$MR_{T(O_2)}$	=	0.215
D_{N_2}	=	2.524×10^{-7}	Q_N	=	6.000
$F_{I(CO_2)}$	=	0.0000	Q_{BN}	=	0.750
$F_{I(O_2)}$	=	0.2100	r_1	=	0.100
$F_{I(N_2)}$	=	0.7900	r_2	=	0.100
(Hb)	=	0.2000			

---

[*]Some parameter values were assigned in writing the system equations, e.g., buffer slope and Haldane effect [Eq. (3.1)], vascular segment volumes [Eqs. (8.10)—(8.14)], controller gains [Eqs. (9.1)—(9.4)], etc.

[**]Although equations distinguish between α values for blood, brain, tissue, and CSF, they were all set equal in this initial exploration.

[***]These values now appear to be too high [37], and will require revision in future explorations.

Appendix C

SAMPLE OF COMPUTER TABULAR PRINT-OUT

TIME 0.0500

ALV RQ 0.8812   RQ DIFF -0.0057

	CO2	2	T2	D E R I V A T I V E S			PCO2	PO2	PN2	(H+)	PH	HBO2
ALVEOLAR	0.0557	0.1388	0.8055	-0.0003	-0.1687	0.1690	39.7114	98.9683	574.3203			
ARTERIAL	0.5749	0.1997	0.0099				39.7114	98.9683	574.3203	38.7691	7.4115	0.1968
BRAIN	0.6503	0.0012	0.0097	0.0000	-0.0000	0.0000	50.2072	36.7730	568.1752	43.5849	7.3607	
TISSUE	0.6245	0.0015	0.0097	0.0000	0.0000	0.0000	44.6013	46.1382	567.6018	40.1557	7.3963	
CSF				0.0081	-0.0007	0.0250	50.1404	36.7779	568.0054	45.8715	7.3385	
V BRAIN	0.6413	0.1343	0.0097				50.2072	36.7730	568.1752	44.2284	7.3543	0.1331
V TISSUE	0.6091	0.1598	0.0097				44.6013	46.1382	567.6018	41.2193	7.3894	0.1583

TRANSPORT TIMES—AB	VB	VT	AT	AO **	VI	VE	Q	QB	DERIVATIVES	
0.1970	0.1113	0.5913	0.3170	0.1877	5.0474	5.0091	6.0055	0.7505	0.2229	0.0537

TIME 0.0600

ALV RQ 0.8850   RQ DIFF -0.0095

	CO2	O2	N2	D E R I V A T I V E S			PCO2	PO2	PN2	(H+)	PH	HBO2
ALVEOLAR	0.0557	0.1371	0.8072	-0.0004	-0.1695	0.1658	39.7090	97.7770	575.5140			
ARTERIAL	0.5750	0.1397	0.0099				39.7090	97.7770	575.5140	38.7642	7.4116	0.1966
BRAIN	0.6503	0.0012	0.0097	0.0001	-0.0000	0.0000	50.2072	36.7840	568.1739	43.5849	7.3607	
TISSUE	0.6245	0.0015	0.0097	0.0000	0.0000	0.0000	44.6014	46.1476	567.6023	40.1557	7.3963	
CSF				0.0081	0.0008	0.0247	50.1404	36.7779	568.0057	45.8716	7.3385	
V BRAIN	0.6413	0.1343	0.0097				50.2072	36.7840	568.1739	44.2290	7.3543	0.1331
V TISSUE	0.6091	0.1598	0.0097				44.6014	46.1476	567.6023	41.2197	7.3849	0.1584

TRANSPORT TIMES—A3	VB	VT	AT	AC **	VI	VE	Q	QB	DERIVATIVES	
0.1970	0.1113	0.5913	0.3170	0.1876	5.0475	5.0104	6.0079	0.7512	0.2524	0.0859

REFERENCES

1. Haldane, J. S., and J. G. Priestley (1905): "The Regulation of the Lung Ventilation," J. Physiol. (London), 32, 225-266.

2. Gray, J. S. (1945): "The Multiple Factor Theory of Respiratory Regulation," AAFSAM Project Report No. 386 (1, 2, 3).

3. Grodins, F. S., J. S. Gray, K. R. Schroeder, A. L. Norins, and R. W. Jones (1954): "Respiratory Responses to CO_2 Inhalation. A Theoretical Study of a Non-linear Biological Regulator," J. Appl. Physiol., 7, 283-308.

4. Grodins, F. S. (1965): "Computer Simulation of Cybernetic Systems," in R. W. Stacy, and B. Waxman (eds.), Computers in Biomedical Research, Vol. 1, Academic Press, New York, 135-164.

5. Defares J. G., H. E. Derksen, and J. W. Duyff (1960): "Cerebral Blood Flow in the Regulation of Respiration," Acta Physiol. Pharmacol. Neerlandica, 9, 327-360.

6. Horgan, J. D., and R. L. Lange (1964): "A Model of the Respiratory Control System Which Includes the Effects of Cerebrospinal Fluid and Brain Tissue," Proceedings of the 17th Annual Conference on Engineering in Medicine and Biology, 6, 10.

7. Clegg, B. R., L. Goodman, and D. G. Fleming (1964): "A Dynamic Model of Respiratory Regulation with Peripheral and Medullary Chemosensors," Proceedings of the 17th Annual Conference on Engineering in Medicine and Biology, 6, 11.

8. Defares, J. G. (1964): "Principles of Feedback Control and Their Application to the Respiratory Control System," in W. O. Fenn, and H. Rahn (eds.), Handbook of Physiology, Vol. 1, Section 3: Respiration, Am. Physiol. Soc., Washington, D. C., 649-680.

9. Milhorn, Howard T., Jr., R. Benton, R. Ross, and A. C. Guyton (1965): "A Mathematical Model of the Human Respiratory Control System," Biophysical J., 5, 27-46.

10. Peters, J. P., and D. D. Van Slyke (1932): Quantitative Clinical Chemistry, Vol. 1, The Williams and Wilkins Co., Baltimore, 518-652, 868-1018.

11. Dantzig, G. B. J. C. DeHaven, I. Cooper, S. H. Johnson, E. C. DeLand, H. E. Kanter, and C. F. Sams (1961): "A Mathematical Model of the Human External Respiratory System," Perspectives in Biology and Medicine, 4, 324-376.

12. Scarborough, W R., R. Penneys, C. B. Thomas, B. M. Baker, Jr., and R. E. Mason (1950) "The Cardiovascular Effect of Induced Controlled Anoxemia," Circulation, 4, 190.

13. Asmussen, E. (1943): "CO_2 Breathing and the Output of the Heart," Acta Physiol. Scand., 6, 176.

14. Richardson, D. W., A. J. Wasserma·, and J. L. Patterson, Jr. (1961): "General and Regional Circulatory Responses to Changes in Blood pH and Carbon Dioxide Tension," $\underline{J.\ Clin.\ Invest}.$, $\underline{40}$, 31-43.

15. Patterson, J. L., Jr. (1965): "Circulation Through the Brain," in T. R. Ruch, and H. D. Patton (eds.), $\underline{Physiology\ and\ Biophysics}$, W. B. Saunders Co., Philadelphia, 950-958.

16. Reivich, M. (1964): "Arterial P_{CO_2} and Cerebral Hemodynamics," $\underline{Am.\ J.\ Physiol}.$, $\underline{206}$, 25-35.

17. Boothby, J. M., and others (1944): $\underline{Handbook\ of\ Respiratory\ Data\ i:\ Aviation}$, OSRD, NRC, Washington, D. C.

18. Mitchell, R. A., H. H. Loeschke, J. W. Severinghaus, B. W. Richardson, and W. H. Massion (1963), "Regions of Respiratory Chemosensitivity on the Surface of the Medulla," $\underline{Ann.\ N.\ Y.\ Acad.\ Sci}.$, $\underline{109}$ (2), 661-81.

19. Lambertsen, C. J. (1963): "Factors in the Stimulation of Respiration by Carbon Dioxide," in D. J. C. Cunningham, and B. B. Lloyd (eds.), $\underline{The\ Regulation\ of\ Human\ Respiration}$, Davis, Philadelphia, 257-276.

20. Dejours, P. (1963): "Control of Respiration by Arterial Chemoceptors," $\underline{Ann.\ N.\ Y.\ Acad.\ Sci}.$, $\underline{109}$ (2), 682-695.

21. Bouverot, P., R. Flandrois, R. Puccinelli, and P. Dejours (1965): "Etude du Rôle des Chémorécepteurs Artériels dans la Regulation de la Respiration Pulmonaire chez le Chien Éveille," $\underline{Arch.\ Int.\ Pharmacodyn}$, 157, 253-271.

22. Bellman, R., J. D. Buell, and R. E. Kalaba (1965): "Numerical Integration of a Differential-Difference Equation with a Decreasing Time Lag," $\underline{Comm.\ of\ A.\ C.\ M}.$, $\underline{8}$, 227-228

23. Bellman, R., and K. L. Croke (1964): $\underline{On\ the\ Computational\ Solution\ of\ a\ Class\ of\ Functional\ Differential\ Equations}$, The RAND Corporation, RM-4287-PR.

24. Bellman, R., and R. E. Kalaba (1965): $\underline{Quasilinearization\ and\ Non-Linear\ Boundary\ Value\ Problems}$, American Elsevier, New York.

25. Pappenheimer, J. R., V. Fencl, S. R. Heisey, and D. Held (1965): "Role of Cerebral Fluids in Control of Respiration as Studied in Unanesthetized Goats," $\underline{Am.\ J.\ Physiol}.$, $\underline{208}$, 436-450.

26. Lambertsen, C. J. (1961): "Chemical Factors in Respiratory Control," in P. Bard (ed.), $\underline{Medical\ Physiology}$, C. V. Mosby Co., St. Louis, 652-653.

27. Mitchell, R. A., C. T. Carman, J. W. Severinghaus, B. W. Richardson, M. M. Singer, and S. Shnider (1965): "Stability of Cerebrospinal Fluid pH in Chronic Acid-base Disturbances in Blood," $\underline{J.\ Appl.\ Physiol}.$, $\underline{20}$, 443-452.

28. Fencl. V , T. B. Miller, and J. R. Pappenhei er (1966): "Studies on the Respiratory Response to Disturbances of Acid-base Balance, with Deductions Concerning the Ionic Composition of Cerebral Interstitial Fluid," Am. J. Physiol., 210, 459-472.

29. Mitchell, R. A., C. R. Bainton, J. W. Seve inghaus, and G. Edlist (1964): "Respiratory Response and CSF pH During Disturbances in Blood Acid-base Balance in Awake Dogs with Denervated Aortic and Carotid Bodies," The Physiologist, 7, 208.

30. Katsaros, B. (1965): "Die Rolle der Chemoreceptoren des Carotisgebiets der narkotisierten Katze für die Antwort der Atmung auf isolierte Anderung der Wasserstoffionen-Konzentration und des CO_2-Drucks des Blutes," Arch. Ges. Physiol., 282, 157-178.

31. Grodins, F. S. (1950): "Analysis of Factors Concerned in Regulation of Breathing in Exercise," Physiol. Rev., 30, 220-239.

32. Grodins, F. S. (1964): "Regulation of Pulmonary Ventilation," The Physiologist, 7, 310-333.

33. Grodins, F. S. (to be published): "Some Simple Principles and Complex Realities of Cardiopulmonary Control in Exercise," Proceedings of the Symposium on Physiology of Exercise, Southwestern Medical School, Dallas, Texas, 1966.

34. Iberall, A. S., and S. Z. Cardon (1965): "Further Study of the Dynamic Systems Response of Some Internal Human Systems," NASA Contractor Report CR-219, May, 1965.

35. Alexander, D. M., and L. Goodman (1964): "Respiratory Gas Exchange Rhythms in Quiescent Man," Proceedings of the 17th Annual Conference on Engineering in Medicine and Biology, 6, 12.

36. Wiedeman, M. P. (1963): "Patterns of the Arteriovenous Pathways," in W. F. Hamilton, and P. Dow (eds.), Handbook of Physiology, Vol. II., Section 2, Chapter 27, American Physiological Society, Washington, D. C., 891-933.

37. Siesjö, B. K. (1966): "Active and Passive Mechanisms in the Regulation of the Acid-base Metabolism of Brain Tissue," in C. McC. Brooks, F. F. Kao, and B. B. Lloyd (eds.), Cerebrospinal Fluid and the Regulation of Ventilation, Blackwell, Oxford, 331-371.

DOCUMENT CONTROL DATA

1. ORIGINATING ACTIVITY	2a. REPORT SECURITY CLASSIFICATION
THE RAND CORPORATION	UNCLASSIFIED
	2b. GROUP

3. REPORT TITLE

MATHEMATICAL ANALYSIS AND DIGITAL SIMULATION OF THE RESPIRATORY CONTROL SYSTE

4. AUTHOR(S) (Last name, first name, initial)

Grodins, Fred S., M.D., June Buell and Alex J. Bart

5. REPORT DATE	6. TOTAL No. OF PAGES	6b. No. OF REFS.
March 1967	56	37

7. CONTRACT OR GRANT No.	8. ORIGINATOR'S REPORT No.
F44620-67-C-0045	RM-5244-PR

9a. AVAILABILITY/LIMITATION NOTICES	9b. SPONSORING AGENCY
DDC-1	United States Air Force Project RAND

10. ABSTRACT

A numerical simulation of the lung-blood-brain-tissue gas transport and exchange system. The basic material balance relationships are expressed in a set of differential-difference equations containing a number of dependent time delays based on blood flow rate and vascular capacity. Other equations define the chemical details of transport and acid-base buffering, concentration equilibria, and blood flow behavior. A control function is given defining the dependence of ventilation of hydrogen ion concentration in the cerebrospinal fluid and oxygen content at the carotid chemoceptors. A 500-statement FORTRAN program simulates the responses of the system to a variety of forcings, including carbon dioxide inhalation, hypoxia at sea level, altitude hypoxia, and metabolic disturbances in acid-base balance. Both dynamic and steady-state behavior were reasonably realistic. About one minute machine time on a CDC 3400 computer was required for every four minutes of simulation. To the authors' knowledge, this is the first digital solution of a set of differential-difference equations whose time delays are themselves dependent variables.

11. KEY WORDS

Mathematics
Computer simulation
Physiology
Bio-engineering
Control theory
Computer graphics
Models